A species-specific, site-sensitive maximum stand density index model for Pacific Northwest conifer forests

Authors: Ryan R. Heiderman<sup>1</sup> and Mark J. Kimsey Jr.<sup>1</sup>

<sup>1</sup>University of Idaho, Department of Forestry, Rangeland and Fire Sciences - Intermountain Forestry Cooperative, 875 Perimeter Dr. MS1133, Moscow, ID 83844-1133, USA.

**Publication**: Canadian Journal of Forest Research • 18 June 2021 • <a href="https://doi.org/10.1139/cjfr-2020-0426">https://doi.org/10.1139/cjfr-2020-0426</a>

#### Abstract

Maximum stand density index (SDI<sub>MAX</sub>) models were developed for important Pacific Northwest conifers of western Oregon and Washington, USA, based on site and species influences and interactions. Inventory and monitoring data from numerous federal, state, and private forest management groups were obtained throughout the region to ensure a wide coverage of site characteristics. These observations include information on tree size, number, and species composition. The effects and influence on the self-thinning frontier of plot-specific factors such as climate, topography, soils, and geology, as well as species composition, were evaluated based on geographic location using a multistep approach to analysis involving linear quantile mixed models, random forest, and stochastic frontier functions. The self-thinning slope of forest stands dominated by Douglas-fir (*Pseudotsuga menziesii* (Mirb.) Franco) was found to be –1.517 and that of stands dominated by western hemlock (*Tsuga heterophylla* (Raf.) Sarg.) was found to be –1.461, leading to regionwide modelled SDI<sub>MAX</sub> values at the 95th percentile of 1728 and 1952 trees per hectare, respectively. The regional model of site-specific SDI<sub>MAX</sub> will support forest managers in decision-making regarding density management and species selection to more efficiently utilize site resources toward healthy, productive forests.

### Résumé

Des modèles d'indice de densité maximale des peuplements (IDP<sub>MAX</sub>) ont été développés pour d'importants conifères de la région du nord-ouest du Pacifique, dans l'ouest de l'Oregon et de l'État de Washington aux États-Unis, en fonction des effets et des interactions entre les stations et les espèces. Des données d'inventaire forestier ont été obtenues de nombreuses unités de gestion forestière fédérales, des États, et privées à travers toute la région pour assurer un large éventail des caractéristiques de station. Ces observations comprennent des informations sur la dimension des arbres, leur nombre et la composition en espèces. Les effets et l'influence sur la ligne d'auto-éclaircie de facteurs spécifiques à la parcelle, comme le climat, la topographie, les sols et la géologie, ainsi que la composition en espèces, ont été évalués en fonction de la localisation géographique en utilisant une approche d'analyse en plusieurs étapes impliquant des modèles linéaires mixtes par quantiles, des fonctions de forêt d'arbres décisionnels et de frontières stochastiques. La pente de la ligne d'autoéclaircie des peuplements forestiers dominés par le douglas de menzies (Pseudotsuga menziesii (Mirb.) Franco) était de -1,517 et celle des peuplements dominés par la pruche de l'ouest (Tsuga heterophylla (Raf.) Sarg.) était de -1,461, ce qui donne des valeurs d'IDP<sub>MAX</sub>, modélisées à l'échelle régionale au 95<sup>e</sup> centile, de respectivement 1728 et 1952 arbres à l'hectare. Le modèle régional d'IDP<sub>MAX</sub> propre à chaque station aidera les aménagistes forestiers à prendre des décisions pour la

<sup>\*</sup> Corresponding Author

gestion de la densité et la sélection des espèces afin d'utiliser plus efficacement les ressources de la station et d'obtenir des forêts saines et productives. [Traduit par la Rédaction]

#### Introduction

Forest stand density is a function of two variables: the number of trees and their size (Zeide 2005). Initially, forest stand development is essentially free of intra- or inter-specific competition, during which time mortality is independent of density (Drew and Flewelling 1977). As trees grow, in particular their canopies, demand on limited forest resources and growing space increases, causing density to become successively lower due to the competitive interaction between individuals and subsequent death of the suppressed (i.e., density-related mortality) (Yoda et al. 1963). A site is fully occupied when the stand has accumulated the maximum attainable biomass at a given stand density where any further growth will incur mortality (Bi et al. 2000). As such, the major drivers of self-thinning in forest stands are self-tolerance and the ability of individuals to acquire site resources through competition for above- and below-ground growing space.

The maximum stand density (SDI<sub>MAX</sub>), or carrying capacity, for a species on a given site is an essential piece of information for assessing site productivity, modelling and predicting stand dynamics, and silvicultural regulation (<u>Pretzsch and Biber 2016</u>). Through silvicultural prescriptions, the density of a forest can be manipulated to achieve specific management objectives (<u>Allen and Burkhart 2019</u>). Manipulation of growing stock allows for the selection of desired species, the lengthening or shortening of a rotation, and the potential to maximize the yield of selected products (<u>Bickford 1957</u>). The ability to predict when natural, density-related mortality will begin to quickly increase is useful to determining the optimal timing and level of thinning regimes of a stand (<u>del Río et al. 2001</u>). The timing of key events such as crown closure and the onset of density-dependent mortality can be anticipated at various levels of density relative to the maximum attainable carrying capacity (<u>Long 1985</u>).

The determination of regional and species-specific SDI<sub>MAX</sub> values for guiding forest management decisions has been, and continues to be, an important subject in forestry research (Zeide 2010). Reineke (1933) plotted the log-log relationship of number of trees against mean diameter to show the upper boundary as a straight, negative-sloping line. A line was visually fit to this outer boundary and the number of trees that intersect at 10 inches (25.4 cm) is what Reineke called the stand density index, where the highest number of trees is considered the maximum attainable density or SDI<sub>MAX</sub>. Stand density index has the benefit of being a standard by which sites can be compared independent of stand age or site quality (Williams 1996). The traditional approach to modelling the self-thinning relationship in forest stands has been to use the Reineke equation of the following form:

$$\log(N) = \beta_0 + \beta_1 \log(QMD) \tag{1}$$

where N is the number of trees per unit area, QMD is the quadratic mean diameter, and  $\theta_0$  and  $\theta_1$  are the slope and intercept parameters to be estimated, respectively. The important features of this linear relationship are the slope of the line, which is the self-thinning rate, and the intercept, which implicitly accounts for site-level variation, including species composition and physical site properties (Andrews et al. 2018). Reineke concluded the slope of the line to be -1.605 and to be invariant to tree species or site quality. Contrary to this belief in a constant slope, many subsequent investigations have revealed systematic variations in slope (Zeide 1987). Although Reineke's -1.605 is a reasonable average over all species, it is probably not quite right for any individual species (Sterba and Monserud 1993). Many

models attempt to determine the growth trajectory and mortality of a stand based on species- and site-specific self-thinning lines that represent maximum carrying capacity.

The intercept and slope of the self-thinning line (eq. 1) varies with site-specific environmental factors such as topography, climate, and soils. Aguirre et al. (2018) state that at large scales, including environmental variables in a density model might be crucial in explaining the variability of the self-thinning line over large environmental gradients. Vospernik and Sterba (2015) found, in general, larger intercepts in stands grown on more productive land. Pretzsch and Biber (2005) describe the limiting boundary, or self-thinning line, as the maximum density of individuals at a given size under optimal site conditions, where any boundary lower than this line would signify a stand under suboptimal growth conditions.

The presence and availability of resources is directly determined by site-specific environmental variables. The amount, spatial distribution, and timing of precipitation and sunlight strongly influence ecosystem structure and functioning (Chapin et al. 2011). Numerous studies have incorporated important climate variables in stand density index modelling efforts (Andrews et al. 2018; Condés et al. 2017; Kweon and Comeau 2017). Moisture and sunlight are the primary drivers of tree growth but are significantly modified by site topography (i.e., slope, aspect, and elevation), as well as soil and geologic properties. A relationship between growth, elevation, and aspect is based on underlying processes related to the influence of elevation and aspect on incoming solar energy and water availability (Coops et al. 2000; Roise and Betters 1981; Stage 1976). Topographic variables have proven important in driving many stand density index models (Kimsey et al. 2019; Weiskittel et al. 2009). Soils influence site quality in many ways, including water holding capacity, nutrient availability, and rooting depth. The significance of water availability on site quality and carrying capacity can be directly influenced by the soils present. Binkley (1984) showed that the most fertile site had the greatest maximum size-density relationship, which dropped off from this ceiling with decreasing fertility. Kimsey et al. (2019) found soil parent material to have an important effect on stand density; in particular, the presence of fine-textured volcanic tephra significantly increased maximum SDI for all species studied. They attribute the increase in carrying capacity on ash-influenced soils to their increased water holding capacity.

Stand composition (i.e., species presence) has been shown to influence the size—density trajectory. Pretzsch (2014) demonstrated how stands of species with varying physiological and morphological traits lead to more efficient, denser crown packing. Pretzsch and Biber (2016) showed that mean stand density was higher in mixed-species stands compared with pure stands, attributing the increase to complementary ecological traits. Woodall et al. (2005) give an example of how inappropriately applying the maximum SDI of a pure lodgepole pine (Pinus contorta Douglas ex Loudon) stand (around 2640 trees per hectare (TPH)) to a stand with only 51% lodgepole could result in a deviation of true maximum SDI of the mixed stand by more than 1000 stems. Kimsey et al. (2019) found significant increases in maximum SDI when shifting from pure stands of Douglas-fir or ponderosa pine (Pinus ponderosa (Douglas ex C. Lawson) var. ponderosa) to mixed stands. This increase was attributed to a mixing of more tolerant species, as shown by the relatively small increase between pure stands of shade-tolerant grand fir and mixed stands of grand fir.

To understand the influence of these biological and environmental effects on the self-thinning line, siteand species-specific covariates are explored in the modelling process. <u>Andrews et al. (2018)</u> used a twostage approach to determine the influence of species and site characteristics on maximum stand density in mixed-species forests of the North American Acadian Region. First, the self-thinning line was fit with plot-specific random intercepts and overall fixed slope, which allowed for a unique maximum SDI to be calculated for each observation. The next step was to use a random forest (RF) approach to determine the influence of the specific plot-level species and site characteristics. Weiskittel and Kuehne (2019), exploring similar mixed-species forests of New England, USA, also used a multistep approach where first a size—density relationship was fit with linear quantile mixed models to estimate slope and plot-specific intercepts, and then RF was utilized to determine the most influential plot-level biotic and abiotic variables. The important variables were then added to the base model in a stepwise fashion until a final model was chosen.

This research project sought to determine whether these proposed methods utilized in other regional modelling efforts are capable of producing accurate SDI<sub>MAX</sub> region-wide models for Pacific Northwest conifer forests and to evaluate if these methods could offer a path towards a standardized approach to nationwide modelling efforts. The overall goal of this study was to utilize the available data and modelling methodologies in the literature to develop maximum stand density index models for important Pacific Northwest conifer species of western Oregon and Washington based on site- and species-specific influences and interactions.

## Materials and methods

## Study area

This analysis covers over 13.6 million hectares of Pacific Northwest forests in western Oregon and Washington, USA, spreading from the southern Klamath Mountains, north along the crest of the Cascade Range, and west through the Willamette Valley and Puget Trough to the Coastal and Olympic ranges reaching the Pacific Ocean. These forests are dominated by coastal Douglas-fir (*Pseudotsuga menziesii* (Mirb.) Franco) stands, western hemlock (*Tsuga heterophylla* (Raf.) Sarg.), and western red cedar (*Thuja plicata* Donn ex. D. Don) climaxes (*Franklin and Waring 1980*). Forest land ownership is diverse and comprises a mixture of federally owned National Forests and Parks, tribal lands, state and local government owned forests, and private forest and timberland held by individuals and timber management organizations. Elevation averages 550 m and varies from sea level to over 4390 m at the top of Mount Rainer. Geology and soils are found in highly varied and complex patterns with extensive influence of volcanic activity (*Franklin and Dyrness 1988*). Thirty-year (1961–1990) mean annual precipitation was 221 cm with a range of 54 to 631 cm. The mean percentage of precipitation during the growing season (May–September) was 15% with a range of 7.5% to 29%. Mean annual temperature from this same period was 9.3 °C with a range of 1 to 13.1 °C.

#### **Data**

Plot data was obtained through a collaborative network of public and private forest land management organizations. Inventory and monitoring plot data represented a range of fixed- and variable-radius sampling methods, each geolocated to allow extraction of desired attributes from spatial layers containing various physiographic metrics. Plot location information, including United States Forest Service (USFS) Forest Inventory and Analysis (FIA) and Field Sampled Vegetation (FSVeg) records, was provided as unfuzzed coordinates. When exact plot location was unavailable, data were rolled up to the stand level (stand shapefiles supplied by data provider) and a stand centroid location was utilized (<10% of the dataset). Each plot record included number of trees per hectare (TPH), quadratic mean diameter

(QMD), and proportion of basal area (BA) by major species groups. Data sources provided species basal area proportions for six species groups: Douglas-fir, western hemlock, western red cedar, red alder (Alnus rubra Bong.), and two other categories of conifer and hardwood. Data screening removed plots with less than 2.54 cm QMD and 24.7 TPH to establish a consistent threshold of diameter and number of trees. Only trees marked as living were included in plot-level estimates. The final dataset consisted of 168 220 unique observations representing the varied range of forest ecotypes across the Pacific Northwest (Fig. 1). The data were broken into two distinct subsets: the first ( $n = 155\,083$ ) are those plots containing at least 10% Douglas-fir by BA, and the second (n = 13 137) consisted of plots with at least 10% western hemlock by BA, which contained no Douglas-fir BA proportion. Summary statistics on plot data are shown in Table 1. Although dominated by western hemlock, the later dataset had a significant BA proportion in secondary species of Pacific silver fir (Abies amabilis Douglas ex J. Forbes), which is rolled into the "other conifer" basal area proportion. This second subset of plots was concentrated in the wetter, climax forest conditions with less extreme heating events found in the Coast Range, Olympic Peninsula, and Northern Cascades; however, each subset covered the range of the study area. These datasets will be referred to as DF-Mix and HemFir, respectively, throughout this paper. Species basal area proportions for each of the two datasets are found in Table 2.

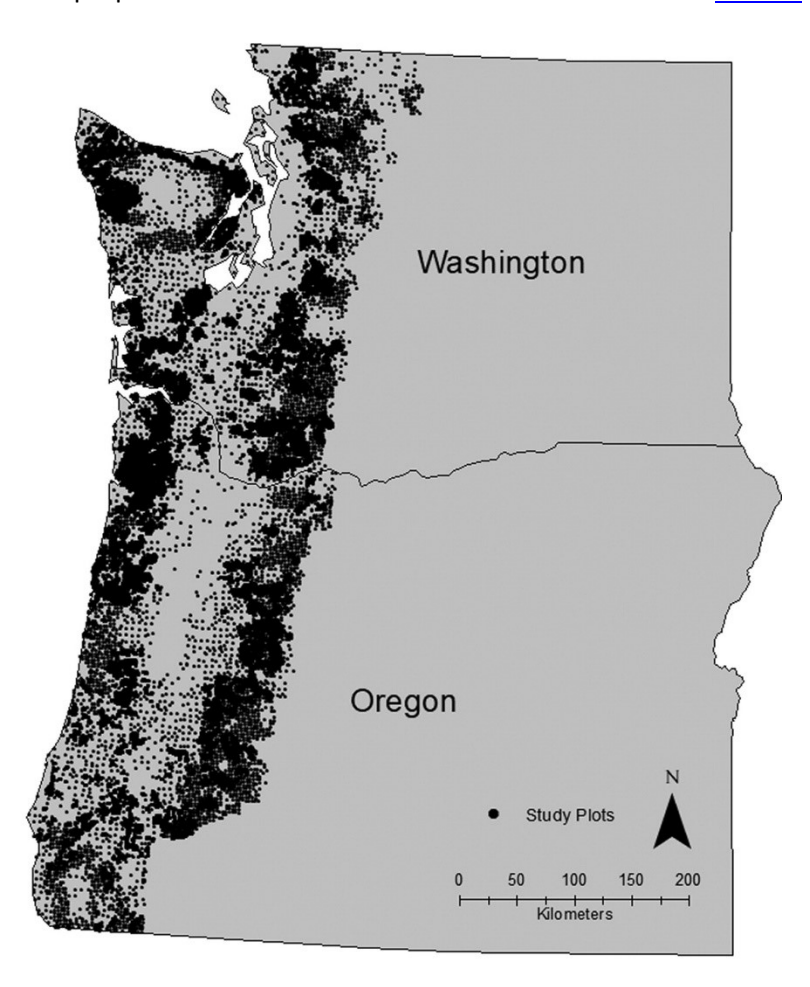


**Fig. 1**. Study locations across Western Washington and Oregon, USA ( $n = 168\ 220$ ). Map was developed in R (<u>R Core Team 2020</u>) with state boundaries from the U.S. Census Bureau TIGER/Line Shapefiles.

**Table 1.** Stand summary characteristics from plot record data used in this study.

Variable	Mean	SD	Minimum	Maximum
DF-Mix $(n = 155 083)$				
Quadratic mean diameter (QMD; cm)	29.3	15.0	2.54	160.5
No. of stems (TPH; trees $ha^{-1}$ ) HemFir ( $n = 13 \ 137$ )	1196.0	2102.4	24.7	56 656.7
Quadratic mean diameter (QMD; cm)	27.6	16.6	2.54	131.3
No. of stems (TPH; trees ha <sup>-1</sup> )	1623.8	2602.2	25.1	38 182.4

**Table 2.** Basal area proportion (%) breakdown of plot data used in this study.

Variable	Mean	SD	Minimum	Maximum
DF-Mix				
Douglas-fir	0.77	0.27	0.10	1
Western hemlock	0.09	0.18	0	0.90
Red alder	0.05	0.15	0	0.90
Western red cedar	0.02	0.07	0	0.90
Other conifer	0.04	0.12	0	0.90
Other hardwood	0.03	0.11	0	0.90
HemFir				
Douglas-fir	0	0	0	0
Western hemlock	0.68	0.30	0.10	1
Red alder	0.13	0.23	0	0.90
Western red cedar	0.04	0.12	0	0.90
Other conifer	0.13	0.23	0	0.90
Other hardwood	0.02	0.09	0	0.90

Topographic attributes were derived from U.S. Department of Agriculture (USDA) and National Resource Conservation Service (NRCS) National Elevation Data 30 m digital elevation models. Slope and aspect were derived using the raster package (<u>Hijmans 2020</u>) available through R 4.0 (<u>R Core Team 2020</u>).

Trigonometric transformations of slope and aspect were utilized to express the influence of these features on climate factors such as moisture and temperature (Roise and Betters 1981). Spatial maps of soil parent materials were derived from U.S. Geological Service (USGS) 1:24 000 geology maps and surficial volcanic ash mantles from the NRCS soil survey geographic database (SSURGO). Major geologic groupings and presence or absence of ash influence were determined similarly to the methods described by Kimsey et al. (2019).

Thirty-year (1961–1990) annual, seasonal, and monthly climate normals were obtained through the ClimateNA v6.11 (Wang et al. 2016) software package using plot-specific latitude, longitude, and elevation. These climate data contained directly calculated and derived variables, as well as various interactions resulting in over 230 climate variables assigned to each record. Some of these important climatic variables can be seen in Table 3.

**Table 3.** Site summary characteristics of plot locations used in this study.

Variable	Mean	SD	Minimum	Maximum
DF-Mix				
LAT (°)	45.18	1.47	42	49
LON (°)	-123.07	0.72	-124.65	-120.73
ELEV (m)	517.20	311.46	0	2098
SLOPE (°)	18.62	10.41	0	59.43
ASPECT (°)	183.37	102.98	0	360
MAT (°C)	9.36	1.30	2.3	13.1
MCMT (°C)	2.56	1.61	-6.3	7.4
MWMT (°C)	16.90	1.33	11.2	21.5
MAP (cm)	214.74	75.22	54.4	571.4
GSP (cm)	32.33	11.44	7.8	85.5
RH (%)	66.15	3.73	52	78
PRATIO	0.15	0.03	0.075	0.29
MAPMCMT	8.25	3.68	<b>-</b> 14.23	24.07
HemFir				
LAT (°)	46.08	1.18	42.70	49
LON (°)	-123.39	0.79	-124.70	-120.77
ELEV (m)	400.18	337.61	0	1574
SLOPE (°)	17.99	10.76	0	56.82
ASPECT (°)	183.82	113.59	0	360
MAT (°C)	9.01	1.21	2.4	11.9
MCMT (°C)	2.73	1.75	-6.5	7.0
MWMT (°C)	15.74	0.86	12.3	20.6
MAP (cm)	267.78	68.72	58.9	630.9
GSP (cm)	42.45	9.87	13.1	92.9
RH (%)	68.99	2.49	55	79
PRATIO	0.16	0.03	0.10	0.26
MAPMCMT	7.25	4.55	-12.03	22.01

Note: LAT, latitude; LON, longitude; ELEV, elevation; MAT, mean annual temperature; MCMT, mean temperature in the coldest month; MWMT, mean temperature in the warmest month; MAP, mean annual precipitation; GSP, growing season precipitation (May–September); RH, mean annual relative humidity; PRATIO, ratio of GSP to MAP; MAPMCMT, interaction between MAP and MCMT ((MAP  $\times$  MCMT)/1000).

### Modeling maximum stand density

The data analysis process involved a multistep approach utilizing linear quantile mixed models and RF in a variable selection process, followed by the development of an SDI<sub>MAX</sub> model using stochastic frontier analysis.

Following the findings of Salas-Eljatib and Weiskittel (2018), linear quantile mixed models (LQMM) were developed with the lqmm package (Geraci 2014) within the R programming environment (R Core Team 2020) to estimate the random plot-specific intercepts and fixed species-specific slope of the self-thinning line based on the Reineke (1933) equation:

$$\ln \text{TPH} = (\beta_0 + k_i) + \beta_1 \cdot \ln \text{QMD}$$
(2)

where TPH is trees per hectare, QMD is quadratic mean diameter (in cm),  $\theta_0$  and  $\theta_1$  are fixed effects parameters, and  $k_i$  is the estimated random effect for plot record i. The random intercept parameter produced unique individual plot level intercept values. The inclusion of a random intercept in the mixed model framework accounts for individual plot level variance, which is influenced by many inherent location factors such as site quality and the myriad possible species compositions found across the study region (Andrews et al. 2018).

Scharf et al. (1998) note that the decision of which quantile best represents the boundary of the data is an arbitrary one and must be made by the investigator. As in Andrews et al. (2018), values from the 90th through the 99th quantile were compared to determine which percentile to utilize. The 95th was chosen as the values produced were reasonable while removing the sensitivity of highly influential observations found at the higher quantiles, as well as unreasonably low values produced at the lower quantiles. Resulting from eq. 2, plot-level SDI<sub>MAX</sub> values for plot *i* can be calculated as

$$SDI_{MAX} = \exp((\beta_0 + k_i) + \beta_1 \cdot ln(25.4))$$
(3)

Individual-plot SDI<sub>MAX</sub> values resulting from the application of <u>eq. 3</u> were then utilized to explore variable influence. Due to the large number of explanatory variables assigned to each plot record, RF analysis (<u>Breiman 2001</u>) with the R package randomForest (<u>Liaw and Wiener 2002</u>) was used as a variable selection process. RF is a machine learning algorithm that constructs an ensemble of decision trees. RF was utilized to understand variable importance in predicting SDI<sub>MAX</sub> and determine the most influential variables to be considered in the final predictive model. RF was run under multiple algorithm parameters utilizing a grid search tuning method to determine the best combination, with a final run of 2500 trees trying approximately one-third of the variables at each node with an 80:20 training—testing split for cross validation. Variable importance plots (varImpPlot) display ranked variables on two criteria based on error and node purity measured by the Gini importance index.

The top variables selected from the RF analysis were then explored using stochastic frontier analysis (SFA). SFA is an econometric approach to expressing the maximum output obtainable from a given input (Aigner et al. 1977). The frontier function is considered stochastic, as opposed to deterministic, due to the two-part error term that allows some observations to lie above the maximum boundary line. The maximum stand density index model can be formulated as follows:

$$\ln \text{TPH} = \beta_0 + \beta_1 \ln \text{QMD} + \beta_i n_i + \varepsilon_i$$
(4)

where

$$\varepsilon_i = v_i + u_i$$
 (5)

TPH is number of trees per hectare, QMD is quadratic mean diameter,  $\theta_0$  is the intercept of the self-thinning line,  $\theta_1$  is the slope of the self-thinning line,  $\theta_i$  are model coefficients for the *i*th site- or species-specific covariate,  $n_i$  represents the value of the *i*th site- or species-specific covariate, and  $v_i$  and  $u_i$  are unobservable random errors (Battese and Corra 1977), where  $v_i$  is assumed identically and

independently distributed as normal with a mean of 0 and variance of  $\sigma_v^2$ . This error term is interpreted as the random effects of both favorable and unfavorable conditions that affect performance, as well as any associated measurement error. The error term  $u_i$  is the non-positive disturbance function assumed half-normal and distributed independently of  $v_i$  with variance of  $\sigma_u^2$ . This error term is interpreted as the deviation from the maximum output. When  $u_i$  is equal to 0, the output has reached maximum.

With respect to the self-thinning boundary, the first error term  $V_i$  is the result of the site factors discussed previously such as climate and topography, as well as the characteristics of the tree species present such as size (QMD), crown architecture, specific gravity, and tolerance to shade, drought, and cold temperatures. This error term also encompasses any measurement error associated with these factors. The second error term reflects the fact that a stand's trajectory has not reached the maximum boundary line, that is, any observation not on the self-thinning boundary line will have  $u_i < 0$ . The model utilizes all observations and is solved by maximum likelihood estimation with the error parameter assumptions as described above.

The variance parameter of the stochastic frontier function is

$$\sigma^2 = \sigma_v^2 + \sigma_u^2 \tag{6}$$

The variance ratio parameter is given by

$$\gamma = \frac{\sigma_u^2}{\sigma_u^2 + \sigma_v^2} \tag{7}$$

where  $\gamma$  lies between 0 and 1. The value of  $\gamma$  can be interpreted as to the applicability of a stochastic frontier function. For example, if  $\gamma = 0$ , then the variance  $\sigma_{\mu}^2 = 0$ , and thus there would be no need to include  $u_i$  in the error term, which would then allow the model to be estimated simply with OLS (<u>Battese and Coelli 1992</u>). As  $\gamma$  approaches 1, the validity of the parameter estimations found by the stochastic frontier function increases.

SFA was run using PROC QLIM in SAS 9.4 (SAS Institute, Inc. 2012) specified as a half normal, production model with the natural log of TPH as the endogenous variable. The top explanatory variables shown as important from the RF analysis were sequentially added and (or) removed depending on Akaike information criterion (AIC) score and  $\gamma$  values. Multicollinearity was assessed among the top variables that were considered in the selection process through Pearson correlation coefficients using the CORR procedure in SAS.

# Independent validation of maximum stand density index model

Final model results were compared against published SDI<sub>MAX</sub> of similar species and region to evaluate reasonableness of predictions and self-thinning line parameter values for slope and intercept. Also, stand growth trajectories of independent, long-term monitoring datasets were utilized to evaluate the predicted self-thinning trajectory. Published tables of remeasured TPH and QMD data from the levels-of-growing-stock (LOGS) Douglas-fir thinning studies (Curtis et al. 1997) and from western hemlock growth and yield trials (Hoyer and Swanzy 1986) were utilized as independent datasets. Stand data were plotted along with the site-specific self-thinning line extracted from the predicted values at the location of these studies. Performance was evaluated based on the trajectory of these data points relative to the predicted self-thinning line.

#### **Results**

#### Quantile regression

LQMM at the 95th quantile with random plot-level intercepts yielded predicted self-thinning slope and intercept of -1.607 (SE = 0.013) and 12.3 (SE = 0.045), respectively, for DF-Mix and -1.544 (SE = 0.017) and 12.227 (SE = 0.060), respectively, for HemFir. The random effects covariance was 0.068 for DF-Mix and 0.096 for HemFir. Mean predicted SDI<sub>MAX</sub> was 1220 TPH (SD = 119) with a range from 464 to 1719 TPH for DF-Mix and 1396 TPH (SD = 151) with a range of 540 to 1916 TPH for HemFir.

#### Influential variables

The RF analysis was utilized for variable selection among the over 250 biotic, climatic, geologic, and topographic factors assigned to each record. Each of the two variable importance measures (error and Gini index) was considered; however, the top 50 variables were fairly consistent between each measure of importance, with 40 of the top 50 in each measure being identical for the DF-Mix dataset and 35 of 50 being identical for the HemFir dataset. The most influential variables were measures of basal area proportions for the following species: western hemlock (WH\_BA), red alder (RA\_BA), western red cedar (RC\_BA), and two "other" categories of conifer (OtherC\_BA) and hardwood (OtherH\_BA), location information (latitude, longitude, and elevation), topographic transformations, and many climatic variables and their interactions describing precipitation and temperature. Similar, but not identical, variables were selected to test in the SFA between the DF-Mix and HemFir datasets.

# Stochastic frontier regression

To begin the process, an initial model of predicting ln(TPH) with the single variable ln(QMD) served as the base model. The base model for DF-Mix and HemFir was considered as having 100% of each species basal area proportion, respectively. Through an iterative process, variables were then introduced to the model and kept or removed based on variable significance (p < 0.0001) and AIC score.

The final models (Table 4) had a  $\gamma$  of 0.924 for the DF-Mix dataset and 0.940 for the HemFir dataset, indicating that SFA was appropriate for modeling the self-thinning boundary line. The self-thinning slope was -1.517 for the DF-Mix model and -1.461 for the HemFir model.

**Table 4.** Summary of frontier model parameters and variance estimates for DF-Mix and HemFir.

Model	Variables	Intercept	Slope	Gamma	AIC
DF-Mix	log(QMD)	12.182 (0.009)	-1.531 (0.003)	0.915	250 321
Reineke					
DF-Mix Full	All	12.202 (0.016)	-1.517 (0.003)	0.924	239 957
HemFir	log(QMD)	12.014 (0.033)	-1.430 (0.010)	0.919	26 624
Reineke					
HemFir Full	All	9.754 (0.177)	-1.461 (0.009)	0.940	26 147

Note: Reineke model only includes intercept and slope, whereas full model includes all chosen species and site variables. Standard errors shown in parenthesis. All variables significant (p < 0.0001).

The final DF-Mix model had the following structure:

```
\begin{split} \text{SDI}_{\text{MAX}} = & \exp(\beta_0 + (\beta_1 \cdot \ln{(25.4)}) + (\beta_2 \cdot \text{WH}_{\text{BA}}) + (\beta_3 \cdot \text{RA\_BA}) + (\beta_4 \cdot \text{RC\_BA}) + (\beta_5 \cdot \text{OtherC\_BA}) + (\beta_6 \cdot \text{OtherH\_BA}) + (\beta_7 \cdot \text{LAT}) \\ & + (\beta_8 \cdot \text{Elev}) + (\beta_9 \cdot \text{tan\_slope\_sin\_aspect}) + (\beta_{10} \cdot \text{cos\_aspect}) + (\beta_{11} \cdot \text{PRATIO}) + (\beta_{12} \cdot \text{MAPMCMT}) + (\beta_{13} \cdot \text{ASH\_Absent}) \\ & + (\beta_{14} \cdot \text{ASH\_Andic}) + (\beta_{15} \cdot \text{ROCK\_type})) \end{split}
```

The final HemFir model had the following structure:

$$\begin{split} \text{SDI}_{\text{MAX}} = \exp(\beta_0 + (\beta_1 \cdot \ln(25.4)) + (\beta_2 \cdot \text{RA\_BA}) + (\beta_3 \cdot \text{RC\_BA}) + (\beta_4 \cdot \text{OtherH\_BA}) + (\beta_5 \cdot \text{LAT}) + (\beta_6 \cdot \text{tan\_slope\_sin\_aspect}) \\ + (\beta_7 \cdot \text{PRATIO}) + (\beta_8 \cdot \text{RH}) + (\beta_9 \cdot \text{TD}) + (\beta_{10} \cdot \text{ASH\_Absent}) + (\beta_{11} \cdot \text{ROCK\_type}) \end{split}$$

The RF variable importance gave high rankings to many of the interaction terms between temperature and precipitation. Often these terms had high multicollinearity between each other. When multiple variables deemed important showed high correlation, only the variable that produced the higher likelihood ratio was kept in the model. For example, in the DF-Mix dataset, RF variable importance showed interactions of both growing season precipitation (GSP) and mean annual precipitation (MAP), with the mean coldest month temperature (MCMT) as having large influence. These two interaction variables, GSPMCMT and MAPMCMT, have a Pearson correlation coefficient of 0.98264; therefore, although both were significant in model development, only MAPMCMT was kept in the model because it produced the larger log likelihood ratio and thus the lower AIC score. Latitude (LAT), which was kept in both the DF-Mix and HemFir models, had the highest Pearson correlation coefficient with PRATIO at 0.58 and 0.52, respectively. Elevation (ELEV), which was kept in the DF-Mix model, had a Pearson correlation coefficient of –0.58 with MAPMCMT. These terms (LAT and ELEV) were kept in the model as they account for other regional, spatial processes such as genetic adaptations of bud phenology and emergence, as well as the effect of day length patterns on other biological developments (St. Clair et al. 2005). No other terms in either model had a Pearson correlation coefficient greater than ±0.5.

In application, if a stand is pure of either Douglas-fir or western hemlock, then the DF-Mix and HemFir models imply 100% basal area proportion of those species, respectively, with other species' basal area proportion values set to 0. As a stand diverges from pure, the additional species' basal area proportion coefficients are introduced. To predict the SDI<sub>MAX</sub> for a stand of 80% Douglas-fir, 15% western hemlock, and 5% other hardwood, 0.15 and 0.05 would be inserted for the values of WH\_BA and OtherH\_BA, respectively, and the remaining 80% Douglas-fir is built into the intercept, with the RA\_BA, RC\_BA, and

OtherC\_BA taking a value of 0. The HemFir model inherently has 0% Douglas-fir basal area and therefore has no coefficient for this species. In the DF-Mix model, mixing of all other species groups increased carrying capacity. In the HemFir model, additional hardwood species mixing had a negative effect on carrying capacity, while the addition of western red cedar, a tolerant species, increased carrying capacity.

Climatic variables were influential in both models (Fig. 2). PRATIO, the ratio of growing season precipitation to annual precipitation (GSP/MAP), was the single most influential climatic variable in each model. The DF-Mix and HemFir model each showed a strong positive effect of having more precipitation during the growing season relative to the annual total. The DF-Mix model included an interaction term between mean annual precipitation and mean temperature in the coldest month (MAPMCMT), which had a negative effect on carrying capacity. This interaction term signified that cooler environments receiving the same precipitation relative to warmer sites can support a higher carrying capacity. Relative humidity (RH) and temperature difference (TD) each had a positive effect on HemFir carrying capacity. The forests that support these climax stands tend to be wetter throughout the year. The TD term was driven mainly by cooler winters rather than hotter summer months, showing that these forests have less extreme heating events and can tolerate the lower temperatures of the winter months.

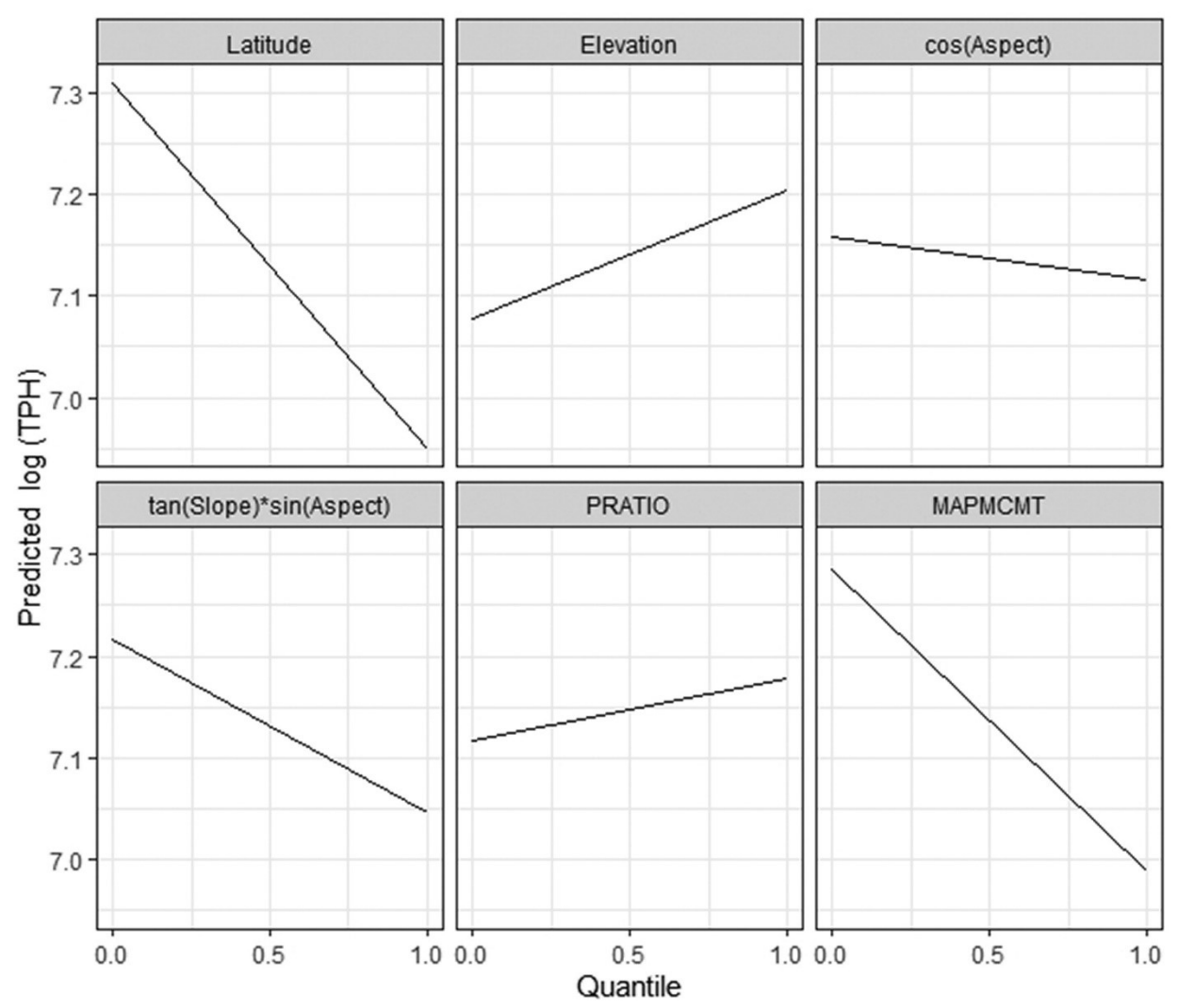


**Fig. 2**. Site effects on DF-Mix predicted maximum density index for the 10th and 90th quantile of each individual site variable while keeping other site variables constant at the 50th quantile. QMD is indexed to 25.4 cm and Douglas-fir basal area proportion is held constant at 100%. QMD, quadratic mean diameter; TPH, trees per hectare.

Elevation had a positive effect in the DF-Mix model, showing that higher elevations support greater carrying capacity. While elevation was shown to be an influential variable in the RF analysis of the HemFir dataset, this variable continuously dropped out during the model building process and was not included in the final HemFir model. Latitude had a negative effect in both models, showing that, with other variables held constant, the forests of the northern latitudes have lower carrying capacity than southern forests. With approximately 7° of latitude between the most southerly and most northerly plot in each dataset, this effect may be capturing the difference in day length with respect to sun angle. The cosine of aspect, a measure of north—south slope effect, had a slight negative effect on DF-Mix carrying capacity as the topography shifted from southerly to northerly. The interaction of tangent of slope and sine aspect, a modification of the east—west slope effect, had a negative effect on SDI<sub>MAX</sub> in both models, giving steeper, eastern-facing slopes a greater carrying capacity than steeper, western-facing slopes. This variable had little effect on flatter topography.

Ash influence (ASH\_ANDIC), or lack thereof (ASH\_ABSENT), was influential in both models. The absence of any underlying volcanic ash negatively affected carrying capacity in each of the DF-Mix and HemFir models. In the DF-Mix model, the presence of andic soil properties increased carrying capacity significantly. Parent materials of sandstone and glacial outwash had a negative effect on DF-Mix and HemFir models, respectively. The geologic and soil variables are binary and receive a value of 1 (present) or 0 (absent) when applying the model.

# **Evaluation of model performance**

The site-specific SDI<sub>MAX</sub> models developed here were compared against published reference curves. Self-thinning slope and intercepts of the 50th and 95th quantiles of growing conditions for each model were determined and plotted against published reference values (<u>Fig. 3</u>). Results from modeling the 95th percentile of modeled SDI<sub>MAX</sub> values for the DF-Mix and HemFir plot data showed 1728 TPH and 1952 TPH, respectively.

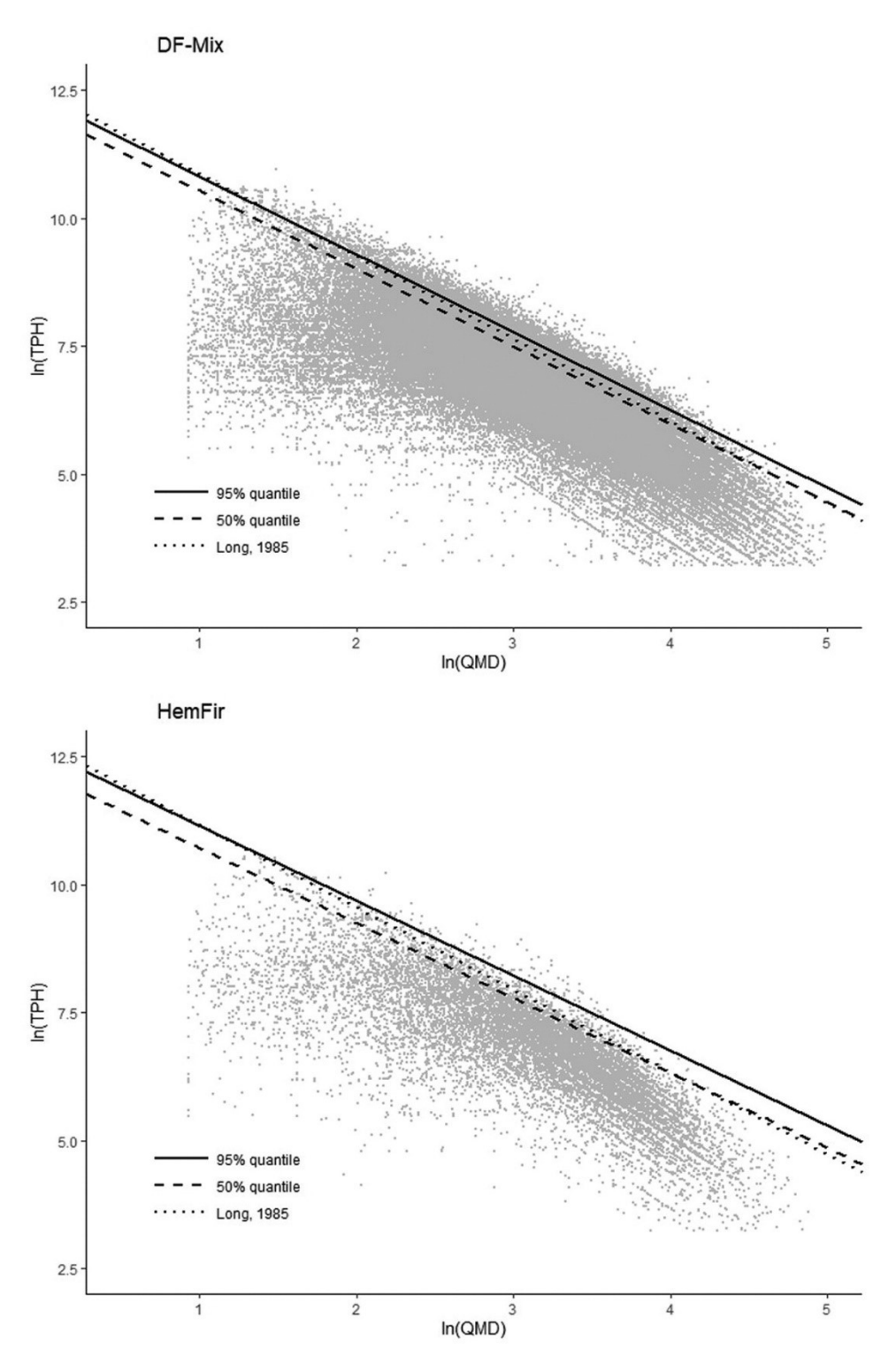


**Fig. 3**. Maximum stand density index frontiers of the 95th (solid line) and 50th (dashed line) quantile of optimal site characteristics. Established regional species-specific maximum density lines (dotted lines) are shown from Long (1985). Dots represent plot-specific size—density relationships. QMD, quadratic mean diameter; TPH, trees per hectare.

When applying the model across the species ranges (expected to make up at least 10% basal area) within the study area (Fig. 4), mean SDI<sub>MAX</sub> values were 1234 TPH for DF-Mix with 100% Douglas-fir basal area and 2068 TPH for HemFir with 100% western hemlock basal area. Predicted SDI<sub>MAX</sub> values at the 0.05 and 0.95 percentiles ranged from 1065 to 1459 TPH for pure Douglas-fir stands and from 1579 to 2644 TPH for pure western hemlock stands. Long (1985) reported SDI<sub>MAX</sub> values of 1450 and 1950 TPH for stands of pure Douglas-fir and western hemlock, respectively.

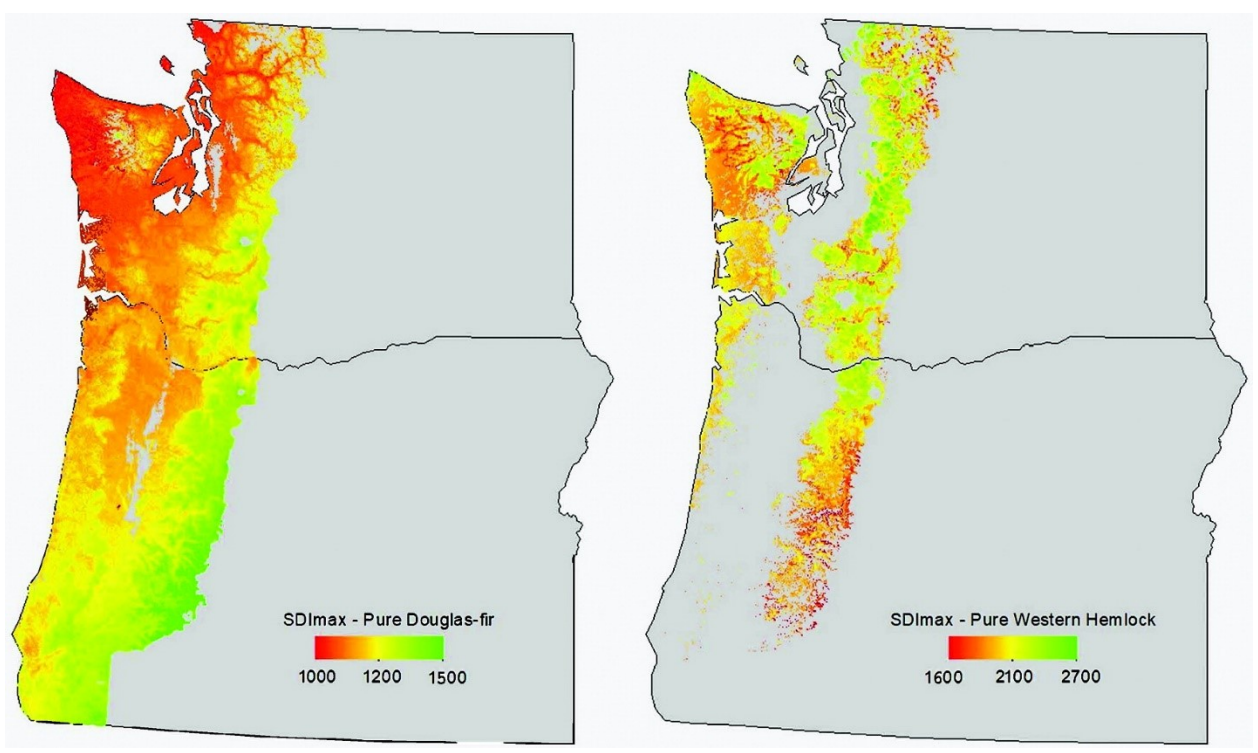


**Fig. 4**. Regional models applied to expected species ranges within the study area with basal area input at 100% for each Douglas-fir and western hemlock within the DF-Mix and HemFir models, respectively. Units represent trees per hectare indexed to 25.4 cm. Output was limited to species range with expected basal area proportion of at least 10%. Map was developed in R (R Core Team 2020) with state boundaries from the U.S. Census Bureau TIGER/Line Shapefiles. SDI<sub>MAX</sub>, maximum stand density index. [Colour online.]

Repeat measurements of control plots from two long-term studies were available to evaluate the modelled self-thinning lines. The first dataset was from the levels-of-growing-stock (LOGS) Douglas-fir thinning trials. The LOGS study had seven sites available in the study region, including Francis (Hoyer et al. 1996), Hoskins (Marshall and Curtis 2002), Rocky Brook (Curtis and Marshall 2009a), Iron Creek (Curtis and Marshall 2009b), Skykomish (King et al. 2002), Clemons (King et al. 2002), and Stampede Creek (Curtis and Marshall 2002). The LOGS study had one western hemlock plot that was also used for evaluating the HemFir model. Data from tables published in these reports were digitized, and site-specific SDI<sub>MAX</sub> values and self-thinning curves were extracted for each location. Plot location information was provided by Oregon State University's Center for Intensive Planted-forest Silviculture group (D. Mainwaring, personal communication). The second dataset came from two western hemlock thinning trials (Clallam Bay and Cascade Head), which were part of a growth and yield study with detailed results published by Hoyer and Swanzy (1986). This report contained detailed location

information to extract modelled SDI<sub>MAX</sub> values at these sites. The results (<u>Fig. 5</u>) of plotting stand development of these repeat-measures datasets against model-predicted, site-specific, self-thinning lines showed an overall good fit of the stand trajectory.

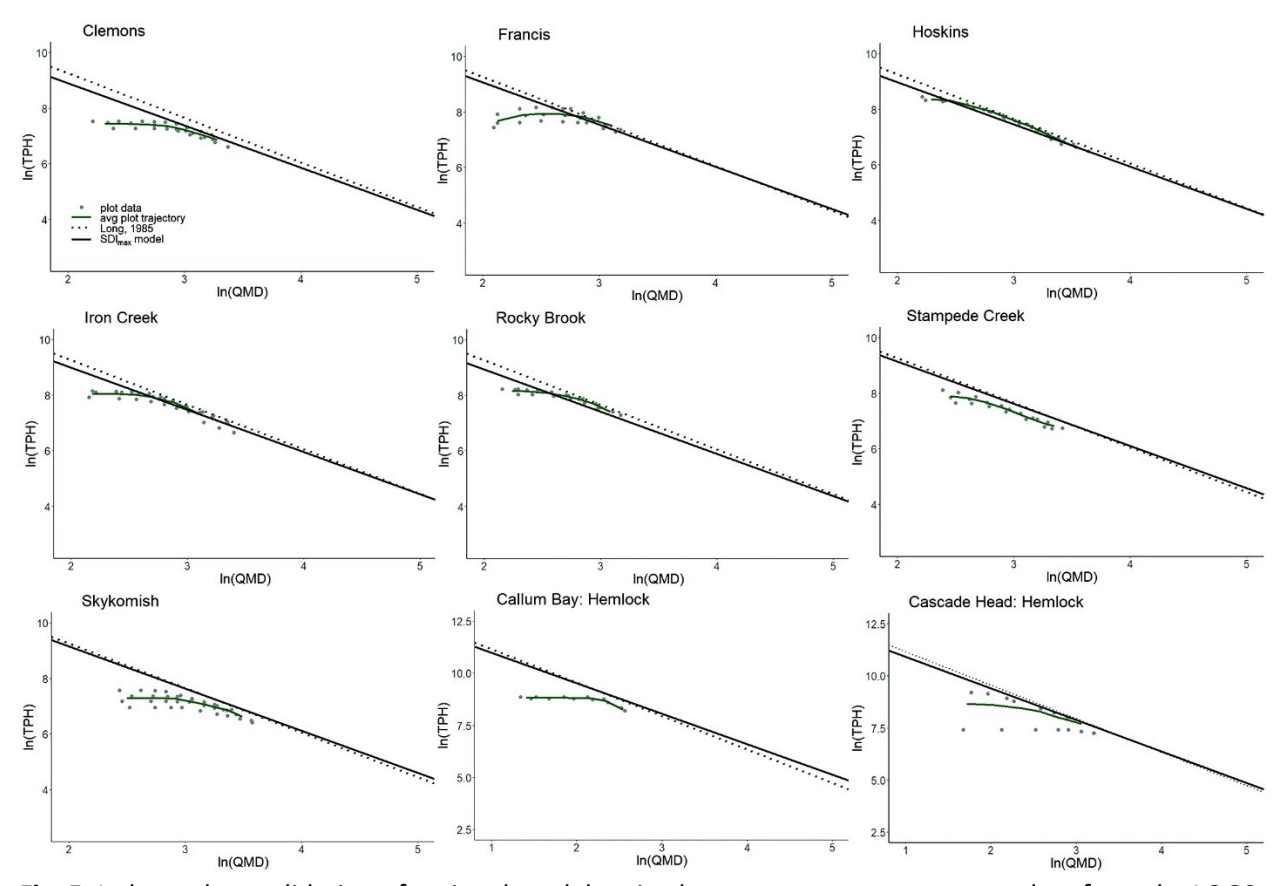


**Fig. 5**. Independent validation of regional models using long-term, repeat-measures data from the LOGS (<u>Curtis 1997</u>) and western hemlock spacing trials (<u>Hoyer and Swanzy 1986</u>). Measured stand size–density trajectories (green line) are plotted against the site-specific modeled SDI<sub>MAX</sub> self-thinning line (solid line). The available dataset (grey dots) with established regional species-specific maximum density frontiers (dotted lines) (<u>Long 1985</u>). SDI<sub>MAX</sub>, maximum stand density index; TPH, trees per hectare; QMD, quadratic mean diameter. [Colour online.]

### **Discussion**

Controlling stand density through silvicultural prescriptions is one of the oldest and most commonly used methods for achieving forest management goals (<u>Allen and Burkhart 2019</u>). Knowledge of stand carrying capacity under given climatic and physiographic conditions is crucial for developing regionally appropriate management guidelines (<u>Condés et al. 2017</u>). Results from this SDI<sub>MAX</sub> modelling analysis have shown the systematic differences of the self-thinning line with respect to varying species composition and site-specific environmental factors. Within the complex landscape of the Pacific Northwest, these results demonstrate the variability of site carrying capacity and the need for site-adapted reference values of maximum density.

Reineke's original analysis utilized only the measures of tree size and number from even-aged monocultures, with no assessment on the impact of environmental factors. It was interesting to note

that the LQMM analysis on only tree size and number of the DF-Mix dataset, which was dominated by records from stands of pure or nearly pure Douglas-fir (median values of 87% Douglas-fir BA proportion), produced a self-thinning slope of -1.607 compared with Reineke's -1.605. While the self-thinning slope may have been similar based solely on the relationship between tree size and number, the subsequent analysis involving environmental variables and, in particular, the introduction of species mixing produce systematic differences in the slope and intercept values.

Utilizing the variable importance results from the RF analysis provided a convenient means of dealing with the large number of potential explanatory variables. This machine learning approach allowed for the identification of predictors to introduce into the regression model. While RF could have potentially been used as the predictive model, we opted for stochastic frontier regression, which allowed for the assignment of coefficients to specific variables. The ability to display the model form with variables and assigned coefficient facilitated technology transfer and application of this model among industry partners.

The results from stochastic frontier regression show a divergence from the self-thinning slope from — 1.605 proposed by Reineke and still utilized for determining SDI today. Stands dominated by Douglas-fir showed a shallower slope of — 1.517, while stands of hemlock—fir showed an even shallower slope of — 1.461. Although not universal (Vospernik and Sterba 2015; Charru et al. 2012), shade-tolerance of species is often thought to have an effect on the self-thinning line (Weller 1987; Jack and Long 1996; Pretzsch and Biber 2016; Kimsey et al. 2019), which is often attributed to the higher "packing density" and ability for shade-tolerant species to fill canopy gaps (Pretzsch 2014). The results presented here show not only a flatter slope for the more shade-tolerant HemFir compared with DF-Mix, but also higher SDI<sub>MAX</sub> values with greater species mixing with complementary ecological traits. For example, in the DF-Mix model, SDI<sub>MAX</sub> increases as a stand moves away from pure, intermediate shade-tolerant Douglas-fir toward a mix with more shade-tolerant western hemlock and western red cedar.

As expected, climate played a significant role in the determination of site-specific SDI<sub>MAX</sub> in both the DF-Mix and HemFir models. Consistency of precipitation, as PRATIO, throughout the growing season had a large positive effect on carrying capacity. This metric signals the droughtiness of the site, with the model showing forests receiving balanced precipitation throughout the year as supporting a greater carrying capacity. Extreme heating events caused a drop in carrying capacity with milder conditions allowing for greater SDI<sub>MAX</sub> in HemFir sites. Throughout the study region, cooler temperatures and greater precipitation allowed for higher carrying capacity. Adapting a species mix at the appropriate density, given expected climatic conditions, can allow for optimization of the stand to capture and utilize site resources.

The influence of particular underlying soil parent material was seen in both models. DF-Mix carrying capacity was negatively affected by sandstone soils. Sandstone-derived soils contain more than 50% sand-sized particles predominantly of quartz and often have low base cation status and nutrient reserve (Buol et al. 2003). HemFir carrying capacity was negatively affected by soils of unconsolidated glacial materials. Glacial-derived soils in the Pacific Northwest are often younger, shallower, and less clay-rich with lower nitrogen content and rapid drainage compared with igneous- or sedimentary-derived soils (Littke et al. 2011).

Site carrying capacity increases when DF-Mix and HemFir stands are found on soils with the presence of volcanic ash. As well, DF-Mix stands growing on sites in the absence of volcanic ash influence were

found to have lower carrying capacity throughout the study region. Soils associated with the volcanic ash tend to have greater nutritional and water holding capacity and have been shown to significantly affect growth and mortality (Coleman et al. 2014; Kimsey et al. 2011).

The range of SDI<sub>MAX</sub> values are in line with results from other published studies from the region (Long 1985; Weiskittel et al. 2009). The higher reported values for the DF-Mix dataset relative to Long (1985) or Reineke (1933) is mainly driven by species mixing, where a stand with a mixture of more shade-tolerant species increases the overall density relative to a stand composed of only less tolerant species. Overall, model evaluation against the long-term datasets demonstrated the importance of site-specific assessment of carrying capacity. There was strong agreement within the Clemons and Iron Creek sites, with the growth trajectory tracking along the predicted self-thinning line. While not unexpected, some sites tracked slightly below, never quite reaching the self-thinning line. These stands tended to self-thin before reaching previously published curves or would curve away from published lines back toward a lower level. Individual stands seldom travel along their self-thinning frontier but are more likely to converge toward them during the self-thinning phase (Vospernik and Sterba 2015). A one-size-fits-all approach to assigning a maximum stand density index solely based on species is not appropriate as can be seen by the varying self-thinning trajectories of these datasets.

The methodology used in this approach was similar to recent analysis and modelling efforts in other regions (Kimsey et al. 2019; Andrews et al. 2018; Ducey et al. 2017). The results presented here show that while the variables chosen for inclusion in the final models may vary between different regions and forest types, the methodology is transferable. The ability to explore a large amount of site- and species-specific variables and determine the most influential for model inclusion is key to developing regionally specific models as variable influence varies between different forested ecosystems. Understanding the influence of climate variables in particular can allow for possible future climate conditions to be assessed within this maximum stand density index modelling framework.

## Conclusion

Site-sensitive, species-specific maximum stand density index models were developed for forest stands of the coastal Pacific Northwest, USA. Many environmental (climate, topography, and underlying soil parent material and ash influence) and biological factors (species mixing) control the self-thinning trajectory of a stand and determine the maximum carrying capacity. Stocking, or relative density, is determined by the ratio of current stand density to the potential maximum and may be utilized to predict certain phases of stand development, in particular the onset of density-dependent mortality. The maximum stand density index serves as a tool for silvicultural prescriptions, including timing and levels of thinning and other density control measures such as initial spacing at planting and species selection. Regionally appropriate models can aid forest managers in decision-making to promote healthy, sustainable, and productive forests.

# Acknowledgements

Data for this research was provided through a collaborative network of regional forest management cooperative members from the Intermountain Forestry Cooperative (IFC) at the University of Idaho and the Center for Intensive Planted-forest Silviculture (CIPS) at Oregon State University. We gratefully acknowledge Robyn Darbyshire and the Region 6 United States Forest Service for providing support and

funding for this project. We also wish to thank the United States Forest Service FIA program for providing unfuzzed data.

#### References

Aguirre A., del Río M., and Condes S. 2018. Intra- and inter-specific variation of the maximum size—density relationship along an aridity gradient in Iberian pinewoods. For. Ecol. Manage. **411**: 90–100.

Aigner D., Lovell C., and Schmidt P. 1977. Formulation and estimation of stochastic frontier production function models. J. Econ. **6**: 21–37.

Allen M. and Burkhart H. 2019. Growth–density relationships in loblolly pine plantations. For. Sci. **65**(3): 250–264.

Andrews C., Weiskittel A., Amato A.W.D., and Simons-Legaard E. 2018. Variation in the maximum stand density index and its linkage to climate in mixed species forests of the North American Acadian Region. For. Ecol. Manage. **417**: 90–102.

Battese G. and Coelli T. 1992. Frontier production functions, technical efficiency and panel data: with application to paddy farmers in India. J. Prod. Anal. **3**: 153–169.

Battese G. and Corra G. 1977. Estimation of a production frontier model: with application to the pastoral zone of eastern Australia. Aust. J. Agric. Econ. **21**: 169–179.

Bi H., Wan G., and Turvey N. 2000. Estimating the self-thinning boundary line as a density-dependent stochastic biomass frontier. Ecology, **81**(6): 1477–1483.

Bickford C. 1957. Stocking, normality, and measurement of stand density. J. For. 55(2): 99–104.

Binkley D. 1984. Importance of size—density relationships in mixed stands of Douglas-fir and red alder. For. Ecol. Manage. **9**(2): 81–85.

Breiman L. 2001. Random Forests. Mach. Learn. 45: 5–32.

Buol, S., Southard, R., Graham, R., and McDaniel, P. 2003. Soil genesis and classification. Iowa State University Press, Ames, Iowa.

Chapin, F., Matson, P., and Vitousek, P. 2011. Principles of terrestrial ecosystem ecology. Springer, New York.

Charru M., Seynave I., Morneau F., Rivoire M., and Bontemps J. 2012. Significant differences and curvilinearity in the self-thinning relationships of 11 temperate tree species assessed from forest inventory data. Ann. For. Sci. **69**: 195–205.

Coleman M., Shaw T., Kimsey M., and Moore J. 2014. Nutrition of Douglas-fir in the Inland Northwest. Soil Sci. Soc. Am. J. **78**(S1): S11–S22.

Condés S., Vallet P., Bielak K., Bravo-Oviedo A., Coll L., Ducey M., et al. 2017. Climate influences on the maximum size—density relationship in Scots pine (*Pinus sylvestris* L.) and European beech (*Fagus sylvatica* L.) stands. For. Ecol. Manage. **385**: 295–307.

Coops N., Waring R., and Moncrieff J. 2000. Estimating mean monthly incident solar radiation on horizontal and inclined slopes from mean monthly temperatures extremes. Int. J. Biometeorol. **44**: 204–211.

Curtis, R., and Marshall, D. 2002. Levels-of-growing-stock cooperative study in Douglas-fir: Report No. 14 — Stampede Creek: 30-year results. USDA Forest Service, Pacific Northwest Research Station, Portland, Ore., Research Paper PNW-RP-543.

Curtis, R., and Marshall, D. 2009*a*. Levels-of-growing-stock cooperative study in Douglas-fir: Report No. 18 — Rocky Brook: 1963–2006. USDA Forest Service, Pacific Northwest Research Station. Portland, Ore., Research Paper PNW-RP-578.

Curtis, R., and Marshall, D. 2009b. Levels-of-growing-stock cooperative study in Douglas-fir: Report No. 19 — Iron Creek: 1966–2006. USDA Forest Service, Pacific Northwest Research Station. Portland, Ore., Research Paper PNW-RP-580.

Curtis R., Marshall D., and Bell J. 1997. LOGS A pioneering example of silvicultural research in coast Douglas-fir. J. For. **95**(7): 19–25.

del Río M., Montero G., and Bravo F. 2001. Analysis of diameter—density relationships and self-thinning in non-thinned even-aged Scots pine stands. For. Ecol. Manage. **142**: 79–87.

Drew R. and Flewelling J. 1977. Some recent Japanese theories of yield–density relationships and their application to Monterey pine plantations. For. Sci. 23(4): 517–534.

Ducey M.J., Woodall C.W., and Bravo-Oviedo A. 2017. Climate and species functional traits influence maximum live tree stocking in the Lake States, USA. For. Ecol. Manage. **386**: 51–61.

Franklin, J., and Dyrness, C. 1988. Natural vegetation of Oregon and Washington. Oregon State University Press, Corvallis, Ore.

Franklin, J., and Waring, R. 1980. Distinctive features of the northwestern coniferous forest: development, structure, and function. *In* Forests: Fresh Perspectives from Ecosystem Analysis, Proceedings, 40th Annual Biological Colloquium. Oregon State University Press, Corvallis, Ore. pp. 59–86.

Geraci M. 2014. Linear Quantile Mixed Models: The 'lqmm' package for Laplace Quantile Regression. J. Stat. Softw. **57**(3): 1–29.

Hijmans, R. 2020. 'raster': geographic data analysis and modeling. R package version 3.3-13. Available from <a href="https://CRAN.R-project.org/package=raster">https://CRAN.R-project.org/package=raster</a>.

Hoyer, G., and Swanzy, J. 1986. Growth and yield of western hemlock in the Pacific Northwest following thinning near the time of initial crown closing. USDA Forest Service, Pacific Northwest Research Station, Portland, Ore., Research Paper PNW-RP-365.

Hoyer, G., Anderson, N., and Marshall, D. 1996. Levels-of-growing-stock cooperative study in Douglas-fir: Report No. 13 — the Francis study: 1963–1990. USDA Forest Service, Pacific Northwest Research Station, Portland, Ore., Research Paper PNW-RP-488.

Jack S. and Long J. 1996. Linkages between silviculture and ecology: An analysis of density management diagrams. For. Ecol. Manage. **86**: 205–220.

Kimsey M., Garrison-Johnston M., and Johnson L. 2011. Characterization of volcanic ash-influenced soils across a geoclimatic sequence. Soil Sci. Soc. Am. J. **75**(1): 267–279.

Kimsey M., Shaw T., and Coleman M. 2019. Site sensitive maximum stand density index models for mixed conifer stands across the Inland Northwest, USA. For. Ecol. Manage. **433**: 396–404.

King, J., Marshall, D., and Bell, J. 2002. Levels-of-growing-stock cooperative study in Douglas-fir: Report No. 17 — the Skykomish study: 1961–93; the Clemons study, 1963–94. USDA Forest Service, Pacific Northwest Research Station, Portland, Ore., Research Paper PNW-RP-548.

Kweon D. and Comeau P. 2017. Effects of climate on maximum size—density relationships in Western Canadian trembling aspen stands. For. Ecol. Manage. **406**: 281–289.

Liaw A. and Wiener M. 2002. Classification and regression by randomForest. R. News, 2(3): 18–22.

Littke K., Harrison R., Briggs D., and Grider A. 2011. Understanding soil nutrients and characteristics in the Pacific Northwest through parent material origin and soil nutrient regimes. Can. J. For. Res. **41**(10): 2001–2008.

Long J. 1985. A practical approach to density management. For. Chron. 61: 23–27.

Marshall, D., and Curtis, R. 2002. Levels-of-growing-stock cooperative study in Douglas-fir: Report No. 15 — Hoskins: 1963–1998. USDA Forest Service, Pacific Northwest Research Station, Portland, Ore., Research Paper PNW-RP-537.

Pretzsch H. 2014. Canopy space filling and tree crown morphology in mixed-species stands compared with monocultures. For. Ecol. Manage. **327**: 251–264.

Pretzsch H. and Biber P. 2005. A re-evaluation of Reineke's rule and stand density index. For. Sci. **51**(4): 304–320.

Pretzsch H. and Biber P. 2016. Tree species mixing can increase maximum stand density. Can. J. For. Res. **46**(10): 1179–1193.

R Core Team. 2020. R: a language and environment for statistical computing. R Foundation for Statistical Computing, Vienna, Austria. Available from https://www.R-project.org.

Reineke L. 1933. Perfecting a stand-density index for even-aged forests. J. Agric. Res. 46(7): 627–638.

Roise J. and Betters D. 1981. An aspect transformation with regard to elevation for site productivity models. For. Sci. **27**(3): 483–486.

Salas-Eljatib C. and Weiskittel A. 2018. Evaluation of modeling strategies for assessing self-thinning behavior and carrying capacity. Ecol. Evol. 8: 10768–10779.

SAS Institute, Inc. 2012. SAS/STAT 9.4 Use's Guide. SAS Institute Inc., Cary, N.C.

Scharf F., Juanes F., and Sutherland M. 1998. Inferring ecological relationships from the edges of scatter diagrams: Comparison of regression techniques. Ecology, **79**(2): 448–460.

Stage A. 1976. An expression for the effect of aspect, slope, and habitat type on tree growth. For. Sci. **22**: 457–460.

St. Clair J., Mandel N., and Vance-Borland K. 2005. Genecology of Douglas-fir in western Oregon and Washington. Ann. Bot. **96**: 1199–1214.

Sterba H. and Monserud R. 1993. The maximum density concept applied to uneven-aged mixed-species stands. For. Sci. **39**(3): 432–452.

Vospernik S. and Sterba H. 2015. Do competition-density rule and self-thinning rule agree? Ann. For. Sci. **72**: 379–390.

Wang T., Hamann A., Spittlehouse D., and Carrol C. 2016. Locally downscaled and spatially customizable climate data for historical and future periods for North America. PLoS ONE, **11**(6): 1–17.

Weiskittel A. and Kuehne C. 2019. Evaluating and modeling variation in site-level maximum carrying capacity of mixed-species forest stands in the Acadian Region and northeastern North America. For. Chron. **95**(3): 171–182.

Weiskittel A., Gould P., and Temesgen H. 2009. Sources of variation in the self-thinning boundary line for three species of varying levels of shade tolerance. For. Sci. **55**: 84–93.

Weller D. 1987. A reevaluation of the –3/2 power rule of plant self-thinning. Ecol. Monogr. 57: 23–43.

Williams R. 1996. Stand density index for loblolly pine plantations in north Louisiana. South. J. Appl. For. **20**(2): 110–113.

Woodall C., Miles P., and Vissage J. 2005. Determining maximum stand density index in mixed species stands for strategic-scale stocking assessments. For. Ecol. Manage. **216**: 367–377.

Yoda K., Kira T., Ogawa H., and Hozumi K. 1963. Self-thinning in overcrowded pure stands under cultivated and natural conditions. J. Biol. **14**: 107–129.

Zeide B. 1987. Analysis of the 3/2 power law of self-thinning. For. Sci. 33(2): 517–537.

Zeide B. 2005. How to measure stand density. Trees, 19: 1–14.

Zeide B. 2010. Comparison of self-thinning models: an exercise in reasoning. Trees, **24**: 1117–1126.